Presented At:

30TH RESEARCH SYMPOSIUM ASNT | EVENTS.
20 - 23 June 2022 | Hilton St. Louis Frontenac | St. Louis, Missouri, USA

Subwavelength Microwave Imaging System using a Negative Index Metamaterial Lens

Srijan Datta, Xiaodong Shi, Yiming Deng and Lalita Udpa

Dept. of Electrical and Computer Engineering, Michigan State University
428 S. Shaw Lane, Room 2120
East Lansing, MI 48824
dattasri@egr.msu.edu

ABSTRACT

This paper describes the design of a subwavelength microwave imaging system using a negative index metamaterial (NIM) lens for nondestructive evaluation (NDE) applications. The imaging system consists of a split ring resonator (SRR)-wire based NIM lens, operating at 6.3 GHz, used in conjunction with a homodyne detection system. Simulation studies of the unit cell design are presented followed by experimental verification of left-handed focusing by the NIM lens with a focal spot of size 0.65λ. A subwavelength hole of diameter 0.25λ in a glass fiber reinforced polymer (GFRP) sample is imaged at a stand-off distance of 1.67λ using the proposed system. High SNR and preservation of polarity and phase information associated with synchronous detection provides a NIM lens imaging system that can be used in the field for rapid inspection at large standoff distances.

Keywords: metamaterials, lenses, microwave imaging, nondestructive evaluation

INTRODUCTION

Microwave imaging sensors can be implemented in the far-field and the near-field modes depending on the distance between the source and test object. In far-field mode, the imaging resolution is limited by the physics of diffraction and objects smaller than wavelength λ cannot be detected. Near-field microwave imaging sensors can provide subwavelength resolution. However, the probe working distance is limited to close proximity of the object (in order of λ/10) for such sensors. Metamaterials with negative refractive index can potentially bridge the gap between the two imaging modes by providing resolution beyond the diffraction limit at greater stand-off distances. A lens made of NIM not only focuses the propagating waves (Figure 1a) but also enhances the amplitude of evanescent waves (Figure 1b), thus allowing for subwavelength imaging using far-field data [1]. A NIM can be implemented as an effective medium using a periodic array of SRR and wire unit cells (Figure 1c). The homogenized negative index behavior of such a periodic structure is described by an effective negative μ (permeability) and ϵ (permittivity) and is given by the relation [2],

(Eq. 1) $\boldsymbol{n = -\sqrt{\mu\epsilon}}$

where n is the effective refractive index.

Presented At:

30TH RESEARCH SYMPOSIUM ASNT | EVENTS.
20 - 23 June 2022 | Hilton St. Louis Frontenac | St. Louis, Missouri, USA

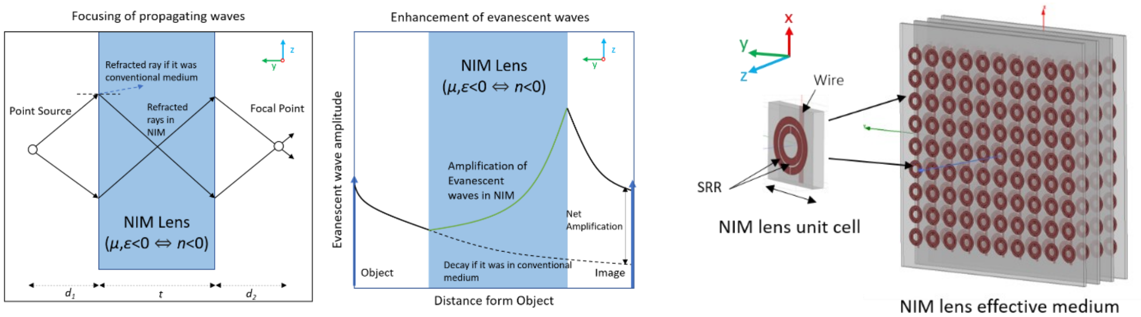

(a) (b) (c)

Figure 1: (a) Focusing of propagating waves from a point source by NIM lens (b) Enhancement of evanescent waves by NIM lens (c) Engineered NIM lens as an array of unit cells

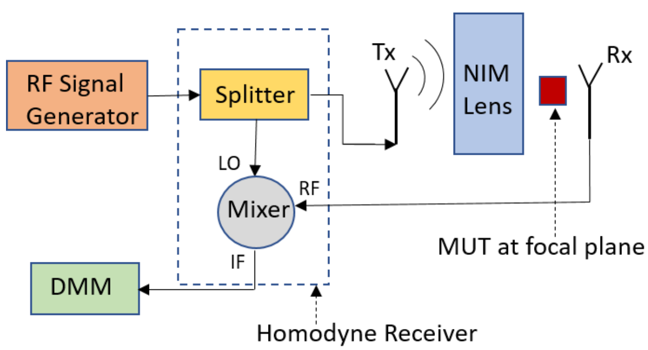

Figure 2: Proposed microwave NDE system for subwavelength imaging

The schematic of the proposed imaging system is shown in Figure 2. The radio frequency (RF) signal generator produces a continuous sinusoidal wave at the desired frequency. The signal is passed through a splitter with one channel connected to the transmitting antenna and the other channel to the local oscillator (LO) port of the mixer. The scattered signal through the lens and test object (placed at the focal plane) is captured by the receiver antenna, which is the RF port of the mixer. The DC signal produced at the intermediate frequency (IF) of the mixer is read by a digital multimeter (DMM) which encodes the phase information of the received signal [3].

NIM UNIT CELL SIMULATION

A NIM can be designed by simulating an infinite array of unit cells using periodic boundary conditions [4]. The unit cell schematic along with the incident wave polarization is shown in Figure 3a. The $\vec{H}$ field is polarized into the plane of the SRRs (z direction) while the $\vec{E}$ field is polarized parallel to the wires (x direction) to generate the required EM response for negative refractive index. A left-handed ($\vec{E}$, $\vec{H}$ and $\vec{k}$ form a left-handed triplet) transmission band is obtained in the frequency region where the refractive index is negative. The dimensional parameters for the unit cell to operate around 6.3 GHz is given by a = 4mm, r = 0.9 mm, t = 0.4 mm, w = 0.4mm, g = 0.2 mm, c = 0.2 mm. FR4 ($\epsilon_r = 4.4$) of thickness 0.6 mm is used as the PCB substrate. The distance between consecutive PCB layers is set to be 3.4 mm. The simulated S parameters for the unit cell design using commercial solver Ansys HFSS is shown in Figure 3b. A transmission band is obtained around 6.3 GHz with a transmission peak of -1.08 dB. To verify the left-handed nature of the transmission band, EM parameter retrieval from the simulated S parameters is performed. The parameter retrieval method is described in the Appendix of [5]. The real part of μ and ϵ are simultaneously negative

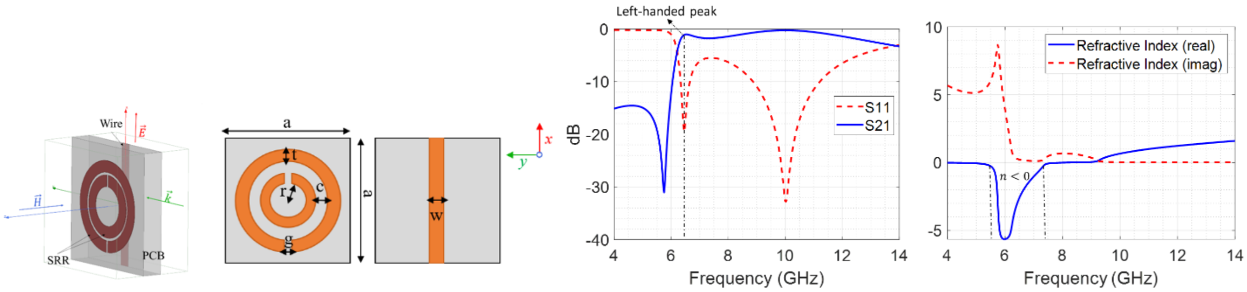

(a) (b) (c)

Figure 3 (a) NIM lens unit cell model with incident wave polarization and unit cell schematic (b) Simulated S parameters using Ansys HFSS (c) Refractive index calculated from simulated S parameters

in this band, rendering the refractive index n to be negative (Equation 1). The refractive index for the proposed NIM lens is -3.33 at the operating frequency of 6.3 GHz (Figure 3c).

EXPERIMENTAL STUDY

A NIM lens, consisting of $N_x = 20$, $N_y = 10$ and $N_z = 30$ unit cells, was fabricated for experimental validation. Figure 4a presents the fabricated metamaterial lens. Each PCB layer consists of 20x10 unit cells and 30 such layers were stacked at intervals of 3.4 mm using 3D printed holder with slots. The final dimensions of the lens are $1.67\lambda \times 0.83\,\lambda\ \times 2.08\lambda$.

Transmission Characteristics

Frequency sweep measurements were performed at the beginning using an Agilent EB070B VNA to experimentally determine the left-handed transmission peak of the fabricated lens. Two horn antennas were used as the transmitter and receiver to ensure correct polarization of the incident EM waves. The antennas were kept at a distance of 20 cm to ensure far-field measurements. A large metallic screen with a window of the size of the lens was used to perform the measurements (Figure 4b). The S_{21} calibrated with free space measurements are shown in Figure 4c. A left-handed peak transmission of -1.5 dB is observed around 6.3 GHz. Conventional right-handed transmission band is obtained above 9.5 GHz. The refractive index of the lens is positive in that frequency region as shown in Figure 3c.

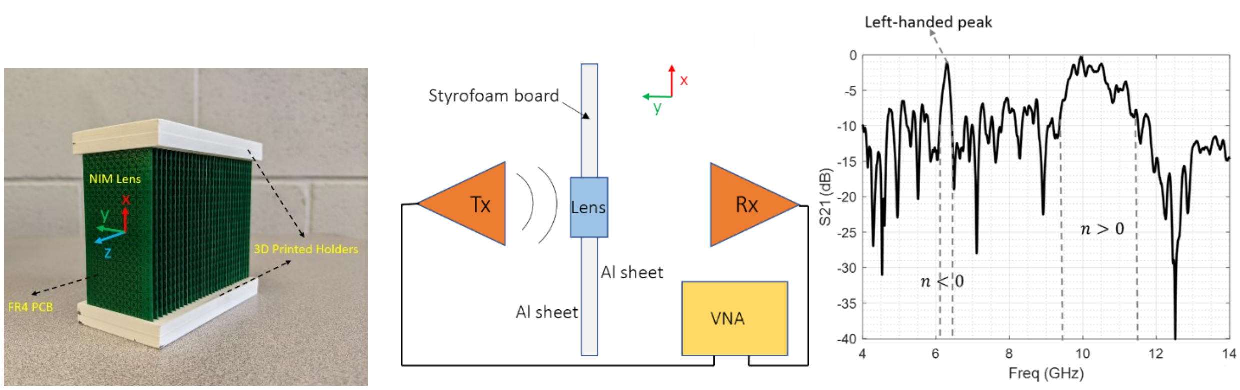

(a) (b) (c)

Figure 4: (a) Fabricated NIM lens (b) Transmission experiment schematic (c) Measured transmission characteristics

Source Imaging

After the left-handed peak frequency was determined, single frequency measurement using synchronous detection was done to provide a low-cost practical imaging system without the need for EM windowing. The setup for the source imaging experiment is shown in Figure 5a. A monopole with resonant frequency of 6.3 GHz was used as source. A monopole antenna produces an azimuthally symmetric field pattern, as does a point source. Left-handed focusing of the incident omnidirectional waves by the NIM lens allows source imaging at the focal plane of the lens. A quarter wavelength monopole was used for measuring the received signal. The receiving probe was mounted on a 2D scanner and moved on the *y*-*z* plane and the received signal distribution was measured. A step size of 5 mm was used in both the *z* and *y* directions. The transmitting monopole was placed at 10 mm from the air–NIM interface. Figure 5b shows normalized received signal distribution. A focal point is observed at a distance 35 mm from the second NIM–air interface. The measured focal spot distance is consistent with NIM lens imaging theory [1]. The source imaging experiment was performed without the NIM lens as well and the results are shown in Figure 5c. The received signal distribution shows the radiation pattern of an omnidirectional source as expected. Figure 5d displays the cross-range intensity profiles for the two cases. The full width at half maxima (FWHM) for the focal spot is found to be 30 mm (0.62λ). The FWHM at the focal plane without the lens is 67 mm (1.39λ) indicating resolution enhancement by a factor of 2.24 ($\Delta_{lens}/\Delta_{free}$) is achieved with the lens.

Subwavelength defect imaging

Next, the capability of imaging subwavelength defects beyond the diffraction limit is demonstrated for NDE applications. The experimental setup is shown in Figure 6a. GFRP samples are used as dielectric test objects. The samples are shown at the inset of the Figure 6a. A hole of diameter 12 mm (0.25λ) is drilled in the sample of dimensions 100 mm x 100 mm x 8 mm. A similar GFRP sample without the drilled hole is used for deriving a baseline or reference signal. The samples are placed at the focal plane of the lens and C scans are performed in the *z*-x plane with a step size of 2 mm. The source to test object distance is 80 mm (1.67λ). The contribution due to the defect is measured by the changes in the test signal relative to the baseline signal.

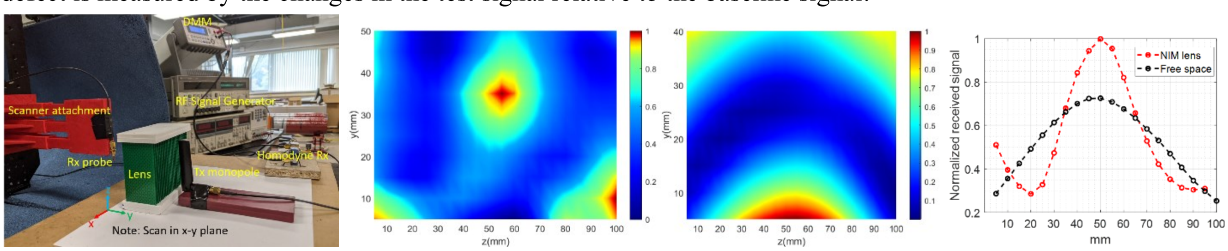

(a) (b) (c) (d)

Figure 5: (a) Source imaging setup (b) Measured intensity distribution with lens (c) Measured intensity distribution without lens (d) Lateral intensity profile comparison at the focal plane for with and without lens.

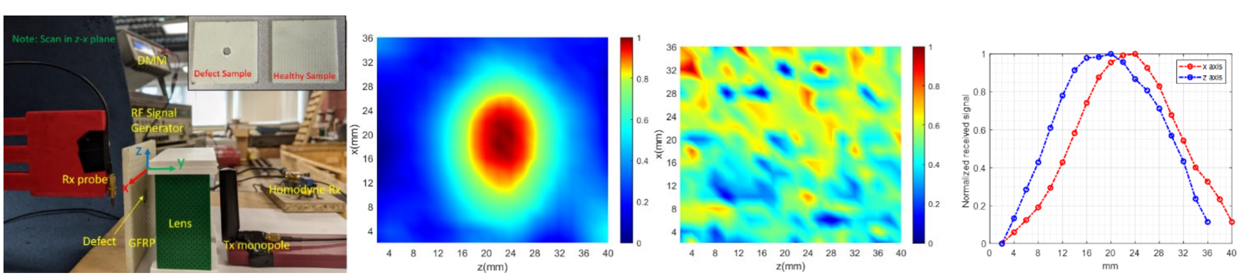

Figure 6: (a) Defect imaging setup (b) Subwavelength defect image with lens (c) Subwavelength defect image without lens (d) Lateral intensity profile of defect image at the focal plane

Presented At:

30TH RESEARCH SYMPOSIUM ASNT | EVENTS.
20 - 23 June 2022 | Hilton St. Louis Frontenac | St. Louis, Missouri, USA

The NDE imaging measurements were repeated without the NIM lens to illustrate that subwavelength defects are not detectable without the lens. The imaging results are displayed in Figure 6. It is seen that the subwavelength defect is undetectable without lens (Figure 6c) and is imaged using the NIM lens (Figure 6b). The lateral intensity profile of the defect image in x and z direction is shown in Figure 6d. The average FWHM of the defect image is 20 mm (0.41λ).

CONCLUSIONS

A metamaterial lens with negative refractive index can provide resolution beyond the diffraction limit at large stand-off distances. This contribution presents the design of a NIM lens imaging system. Unit cell simulation study of the NIM lens is reported followed by experimental validation. Homodyne detection scheme is used in conjunction with the lens to provide a practical NDE imaging system. Source imaging as well as subwavelength defect imaging results with and without the NIM lens are presented. The resolution of NIM lenses is limited by the inherent losses in the design. Future work will include design of low loss metamaterial lenses to further enhance subwavelength imaging resolution.

ACKNOWLEDGEMENT

The work was sponsored by the ASNT fellowship award 2021.

REFERENCES

[1] Pendry, J. B. (2000). Negative refraction makes a perfect lens. *Physical Review Letters*, *85*(18).

[2] Smith, D. R., Padilla, W. J., Vier, D. C., Nemat-Nasser, S. C., & Schultz, S. (2000). Composite Medium with Simultaneously Negative Permeability and Permittivity. *Physical Review Letters*, *84*(18), 4184–4187.

[3] Noll, D. C., Nishimura, D. G., & Macovski, A. (1991). Homodyne Detection in Magnetic Resonance Imaging. *IEEE Transactions on Medical Imaging*, *10*(2), 154–163.

[4] Datta, S., Shi, X., Mukherjee, S., Deng, Y., & Udpa, L. (2020). Model-Based Study of a Metamaterial Lens for Nondestructive Evaluation of Composites. *Journal of Nondestructive Evaluation, Diagnostics and Prognostics of Engineering Systems*, *3*(4).

[5] Datta, S., Mukherjee, S., Shi, X., Haq, M., Deng, Y., Udpa, L., & Rothwell, E. (2021). Negative index metamaterial lens for subwavelength microwave detection. *Sensors*, *21*(14), 1–16.